ELSEVIER

Biochimica et Biophysica Acta 1274 (1996) 9–20

BBA Biochimica et Biophysica Acta

Axial heme ligation in the cytochrome bc_1 complexes of mitochondrial and photosynthetic membranes. A near-infrared magnetic circular dichroism and electron paramagnetic resonance study

Michael G. Finnegan [a], David B. Knaff [b,c], Hong Qin [b], Kevin A. Gray [d], Fevzi Daldal [d], Linda Yu [e], Chang-An Yu [c], Susan Kleis-San Francisco [c], Michael K. Johnson [a,*]

[a] *Department of Chemistry and Center for Metalloenzyme Studies, University of Georgia, Athens, GA 30602, USA*
[b] *Department of Chemistry and Biochemistry, Texas Tech University, Lubbock, TX 79409, USA*
[c] *Institute for Biotechnology, Texas Tech University, Lubbock, TX 79409, USA*
[d] *Department of Biology, Plant Science Institute, University of Pennsylvania, Philadelphia, PA 19104, USA*
[e] *Department of Biochemistry and Molecular Biology, Oklahoma State University, Stillwater, OK 74078, USA*

Received 31 July 1995; accepted 13 November 1995

Abstract

The combination of EPR and low-temperature near-IR magnetic circular dichroism spectroscopies have been used to investigate the axial ligation of the cytochromes in the cytochrome bc_1 complexes from bovine heart mitochondria, *Rhodobacter capsulatus*, *Rhodobacter sphaeroides*, and *Rhodospirillum rubrum*, and the purified cytochromes c_1 from bovine heart mitochondria, *Rb. capsulatus* and *Rb. sphaeroides*. The possibility of axial ligation of cytochrome c_1 by the amino terminus of the polypeptide was also assessed by acetylating the N-terminus of *Rb. capsulatus* cytochrome c_1 and comparing the properties of the acetylated and unmodified samples. The results are consistent with *bis*-histidine axial ligation for the high- and low-potential *b*-type cytochromes and histidine/methionine axial ligation for the c_1-type cytochrome in the intact cytochrome bc_1 complexes. Purified samples of cytochrome c_1 are mixtures of two forms, one with histidine/methionine and the other with *bis*-histidine axial ligation. The form with *bis*-histidine axial ligation is also assembled in the M183L mutant of the *Rb. capsulatus* cyt bc_1 complex in which the methionine residue coordinating cyt c_1 is replaced by a leucine. The *bis*-histidine form appears to be an artifact of dissociation of cytochrome c_1 from the cytochrome bc_1 complex and is greatly enhanced particularly in the bacterial cytochromes c_1 by sample handling and the addition of 50% (v/v) ethylene glycol or glycerol.

Keywords: Cytochrome bc_1; Cytochrome c_1; EPR; Magnetic circular dichroism; Mitochondrion; Photosynthetic bacterium

1. Introduction

Ubiquinol-cytochrome *c* oxidoreductases (cyt bc_1 complexes) are oligomeric electron transfer enzymes located in the inner membrane of mitochondria and the plasma membrane of bacteria (for recent reviews see Refs. [1–6]). They play key roles in respiration in eukaryotic cells and in respiration, cyclic photosynthetic electron transfer, denitrification, and nitrogen fixation in a diverse range of bacterial cells. In all cases they catalyze electron transfer from ubiquinol to cyt *c* or c_2, which is coupled to the generation of the electrochemical potential gradient across the membrane, thereby providing an energy source for ATP synthesis and other energy-requiring processes. The mechanism of this energy transduction has been extensively investigated and some form of protonmotive Q-cycle mechanism is currently accepted by most researchers. While there is as yet no high-resolution crystal structure for any cyt bc_1 complex, the combined efforts of numerous groups have produced a consistent picture of the subunit structure as well as the type and spatial arrangement of the redox centers. The cyt bc_1 complexes of photosynthetic bacteria have generally proven simpler to study than the functionally equivalent mitochondrial com-

Abbreviations: cyt, cytochrome; cytochrome bc_1 complex, ubiquinol-cytochrome *c* oxidoreductase; DMG, decanoyl-*N*-methylglucamide; HALS, highly anisotropic low-spin; (VT)MCD, (variable-temperature) magnetic circular dichroism; ENDOR, electron-nuclear double resonance; λ_{CT}, wavelength of the MCD maximum of the porphyrin(π)-to-Fe(III) charge transfer bands in the near-IR MCD spectrum.

* Corresponding author. Fax: +1 706 5429454; e-mail: johnson@sunchem.chem.uga.edu.

SSDI 0005-2728(95)00155-7

plexes, because of their relatively simple subunit composition (three or four subunits compared to ten in the mitochondrial cyt bc_1 complex) [3,4,7], the availability of mutants [3,4], and the ability to monitor the passage of a single electron through the complex in situ after activation of the photosynthetic electron flow by a short laser flash [7,8].

Cyt bc_1 complexes contain four electron-carrying prosthetic groups [1–6]. The cyt b subunit contains two inequivalent b-type hemes (designated b_H and b_L to distinguish the higher and lower potential hemes). Cyt c_1 contains a single c-type heme that is covalently bound via two thioether linkages formed by reaction of heme vinyl groups with two cysteine residues. The Rieske subunit contains a single Rieske-type [2Fe-2S] iron-sulfur cluster. The specific residues that ligate the Fe atoms of these prosthetic groups have been tentatively identified on the basis of spectroscopic and/or mutagenesis results. EPR and ENDOR studies coupled with mutagenesis results have identified the two histidines and two cysteines that ligate the reducible and non-reducible Fe sites of the [2Fe-2S] cluster, respectively [9–11]. The HALS-type EPR signals of cyt b_H and b_L in mitochondrial and bacterial cyt bc_1 complexes have been interpreted in terms of *bis*-histidyl coordination with near perpendicular arrangements of the imidazole rings [12]. This is supported by room-temperature near-IR MCD studies of cyt b purified from yeast mitochondria [13] and mutagenesis studies of the four totally conserved histidines in the *Rhodobacter sphaeroides* cyt bc_1 complex [14]. While histidine/methionine axial ligation appears most likely for cyt c_1 in both mitochondrial and photosynthetic membranes, not all the data is consistent with this assignment and definitive spectroscopic data is not available for the photosynthetic systems.

EPR and near-IR MCD studies of oxidized cyt c_1 purified from yeast mitochondria revealed a mixture of two species with the dominant component having histidine/methionine axial ligation based on the wavelength of the MCD maxima of the porphyrin (π)-to-iron charge transfer bands (λ_{CT}) [13]. The EPR spectra of *Rb. sphaeroides* cyt c_1, both as isolated and in the intact cyt bc_1 complex, are also consistent with this assignment [15,16]. However, the near absence of the characteristic methionine-to-iron charge transfer band at 695 nm and the recent resonance Raman studies of cyt c_1 isolated from bovine heart and *Rb. sphaeroides* suggest significant differences in axial ligation compared to cyt c at neutral pH [17]. Moreover, recent crystallographic studies for the functionally related cyt f of the chloroplast b_6f complex have revealed novel axial heme ligation involving histidine and the amino terminus of the polypeptide [18]. Perhaps the most convincing support for histidine/methionine axial ligation for cyt c_1 comes from sequence comparisons and mutagenesis studies. In addition to the CXXCH heme binding domain which is present in all c_1- and f-type cytochromes sequenced thus far, a methionine (M183 in the numbering of the mature protein from *Rhodobacter capsulatus*) is conserved in all cyts c_1, but not in cyts f [19]. Furthermore, mutation of this residue to a leucine in *Rb. capsulatus* (M183L mutant), resulted in a complete loss of catalytic activity, concomitant with a dramatic shift in the midpoint potential of cyt c_1 ($\Delta E_m = -390$ mV) [19]. This is consistent with the commonly held view that methionine coordination is responsible for the high redox potential of cyt c_1 (typically around +300 mV *versus* NHE). A similar loss of catalytic activity has been reported for the equivalent mutation in yeast cyt c_1, although in this case the heme moiety was not assembled [20].

Here we report a systematic study of the axial ligation of heme prosthetic groups in cyt bc_1 complexes from bovine heart mitochondria and three photosynthetic bacteria, *Rb. capsulatus*, *Rb. sphaeroides*, and *Rhodospirillum rubrum*, using the combination of low temperature near-IR-MCD and EPR spectroscopies. In addition, the consequences of the M183L mutation on the axial ligation of cyt c_1 in *Rb. capsulatus* have been investigated. Both the intact cyt bc_1 complexes and the purified cyts c_1 (except *R. rubrum* cyt c_1) have been investigated. Taken together, these two spectroscopic methods provide a discriminating method for determining axial heme ligation [13,21–23] and near-IR-MCD is particularly adept at identifying hemes with histidine/methionine axial ligation [24,25]. The possibility of axial ligation of cyt c_1 by the amino terminus of the polypeptide as found in cyt f, was also assessed by acetylating the N-terminus of *Rb. capsulatus* cyt c_1 and comparing the properties of the acetylated and unmodified samples. The results support histidine/histidine and histidine/methionine axial ligation for the b-type and c_1-type hemes in the intact complexes, respectively. However, they also reveal that cyt c_1 can be converted to an alternative form with *bis*-histidine axial ligation, and that this form is particularly prevalent in purified samples of bacterial cyts c_1.

2. Materials and methods

The cyt bc_1 complexes from bovine heart mitochondria, wild-type *Rb. capsulatus*, *R. rubrum*, *Rb. sphaeroides*, and the *Rb. capsulatus* M183L cyt c_1 mutant were prepared and assayed for quinol:cyt c oxidoreductase activity as previously described [16,19,26–28]. Cyt c_1 was isolated from the cyt bc_1 complex of bovine heart mitochondria [29], *Rb. capsulatus* [19] and *Rb. sphaeroides* [30] according to the published procedures. In the case of *Rb. capsulatus* cyt c_1, an additional gel filtration chromatography step on a Pharmacia Superdex-75 HR 10/30 column was utilized to remove a residual amount of Rieske protein. Concentrations of the cyt bc_1 complexes and cyt c_1 samples were determined optically using the published extinction coefficients [16,19,26–30]. Purified *Rb. capsulatus* cyt c_1 was acetylated using the procedure developed by

Takemori et al. [31] for the acetylation of equine cyt *c*. The cyt c_1 samples used for these experiments were judged to be at least 95% pure based on gel electrophoresis and amino acid sequencing results. A 140-fold molar excess of acetic anhydride was added gradually, with continuous stirring, to a sample of cyt c_1 to which sodium acetate had been added (final concentration equivalent to 50% saturation) and which was maintained at 0°C. After 30 min, the sample was dialyzed against 10 mM sodium phosphate buffer (pH 7.4) for 12 h at 4°C with four changes of buffer. As for the unmodified sample, the acetylated sample was concentrated using an Amicon ultrafiltration cell (YM10 membrane) and stored at −20°C. Redox titrations of unmodified and acetylated *Rb. capsulatus* cyt c_1 were carried out using a Johnson Research Foundation spectrophotometer according to the method of Dutton [32], with the apparatus and data analysis techniques described previously [26]. Samples of unmodified and acetylated *Rb. capsulatus* cyt c_1 for amino acid sequencing were applied to Applied Biosystems ProSpin™ sample preparation cartridges containing a ProBlot™ poly(vinyl difluoride) (PVDF) membrane following protocols supplied by the manufacturer. The PVDF membranes with bound protein were recovered and placed in Porton Instruments Model PI2020 Protein Sequencer with an on-line Beckman Gold HPLC system for N-terminal sequence analyses. Isoelectric focusing was performed using a Pharmacia Phast System and "Phast" gels (p*I* 3–9).

Samples were oxidized with ferricyanide prior to spectroscopic studies and excess ferricyanide was removed by Amicon ultrafiltration during exchange from the H_2O to D_2O buffering medium (required for near-IR MCD studies). Low-temperature absorption was recorded on the samples used for VTMCD studies using a Shimadzu UV3101PC UV/visible/near-IR spectrophotometer fitted with an MPC 3100 large cell compartment that accommodates the MCD magnet in the light path. Samples for low-temperature absorption and near-IR-MCD studies contained 50–60% (v/v) d_2-ethylene glycol or d_3-glycerol to enable optical quality glasses to form on freezing. Near-IR and UV/visible MCD spectra were recorded using a Jasco J-730 and J500C spectropolarimeter, respectively, interfaced to an Oxford Instruments SM3 superconducting magnet (magnetic field, 0–5 T; sample temperature 1.5–300 K) using the protocols described elsewhere [33,34]. EPR spectra were recorded on a Bruker Instruments ESP 300D X-band spectrometer equipped with an Oxford Instruments ESR 900 liquid helium flow cryostat.

3. Results

3.1. Spectroscopic studies of bovine heart mitochondrial cyt bc_1 complex and cyt c_1

Near-IR VTMCD spectra for oxidized bovine heart cyt bc_1 complex and isolated cytochrome c_1 at p*D* 8 and 10 are shown in Fig. 1. Absorption spectra of the samples in the MCD magnet were measured at 1.6 K to assess the oxidation state of cyt c_1. In all cases cyt c_1 was judged to be fully oxidized. EPR spectra for the identical samples used in the VTMCD studies are shown in Fig. 2. The EPR spectra of the cyt bc_1 complex and cyt c_1 at p*D* 8 are in excellent agreement with the previously published data [12] and the features at $g = 3.79$, 3.43, and 3.37 (ascorbate reducible component underlying the $g = 3.43$ feature in the cyt bc_1 complex spectrum) are assigned to the low field components of the low-spin Fe(III) resonances of cyt b_L, cyt b_H, and cyt c_1, respectively. In addition to the $g = 3.37$ feature, isolated samples of bovine heart cyt c_1 also exhibited a slower relaxing resonance $g = 2.95$, 2.25, 1.53 that is more pronounced at higher temperatures and/or lower microwave powers, see inset in Fig. 2. This additional species was evident in samples of yeast cyt c_1 [13] and is clearly present (although not commented on) in the

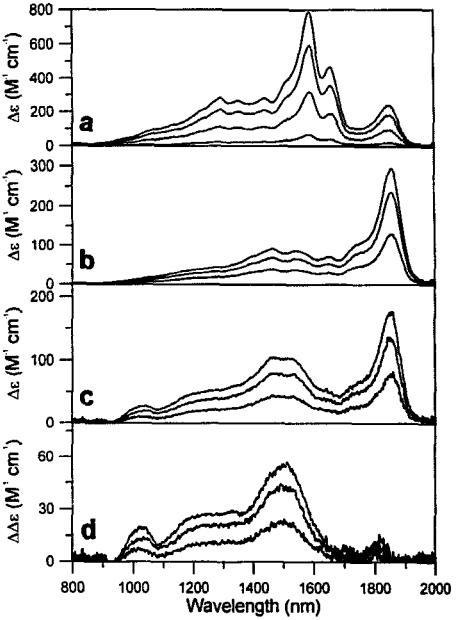

Fig. 1. VTMCD spectra of bovine heart cyt bc_1 complex and isolated cyt c_1. (a) Cyt bc_1 complex, 63 μM in Tris-DCl buffer (p*D* 7.8), with 0.7% DMG and 50% d_2-ethylene glycol. Spectra recorded with an applied magnetic field of 4.5 T at 1.71 K, 4.22 K, 9.6 K, and 52 K. (b) Cyt c_1, 285 μM in 15 mM KP_i/d_2O buffer (p*D* 8.0), with 50% d_2-ethylene glycol. Spectra recorded with an applied magnetic field of 4.5 T at 1.88 K, 4.22 K and 9.3 K. (c) Cyt c_1, 103 μM in 25 mM CAPS/d_2O buffer (p*D* 10.0), with 50% d_2-ethylene glycol. Spectra recorded with an applied magnetic field of 4.5 T at 1.72 K, 4.22 K, and 9.6 K. (d) Difference spectrum, (c) minus (b) at equivalent temperatures. The difference spectra were constructed to minimize the intensity at 1850 nm. All MCD bands increase in intensity with decreasing temperature.

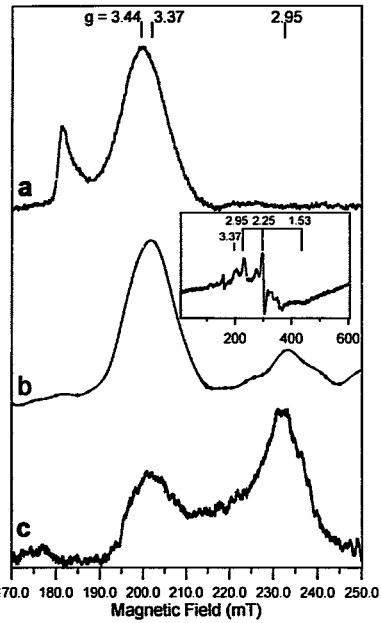

Fig. 2. EPR spectra of bovine heart cyt bc_1 complex and isolated cyt c_1. (a) Cyt bc_1 complex. (b) Cyt c_1 at pD 8.0. (c) Cyt c_1 at pD 10.0. The spectra were recorded at 10 K and the instrument settings were: microwave power, 10 mW; modulation amplitude, 0.64 mT; microwave frequency 9.6 GHz. The inset shows an expanded field range for the cyt c_1 sample at pD 8.0 at a temperature of 35 K and a microwave power of 100 mW. The samples are described in Fig. 1.

previously published spectra of bovine cyt c_1 [12]. The relative concentration of the $g = 3.37$:$g = 2.95$ species was estimated to be 4:1 by integration of the low field absorption-shaped components under non-saturating conditions and correcting for the different transition probabilities according to the published procedure [35]. Raising the pD to 10. resulted in an irreversible increase in the $g = 2.95$ species, see Fig. 2, and the relative concentrations of the $g = 3.37$:$g = 2.95$ species was estimated to be 2:3 at pD 10.

The changes in the EPR accompanying isolation of cyt c_1 and increasing the pD from 8 to 10 are mirrored by changes in the porphyrin(π)-to-Fe(III) charge transfer bands in the near-IR MCD spectra, see Fig. 1. Low-spin Fe(III) hemes have two porphyrin(π)-to-Fe(III) charge transfer bands in the near-IR region. Both exhibit positively signed MCD transitions and the lower energy component almost invariably has the larger intensity [13,21–23]. The energy of these transitions, as assessed by the wavelength of the MCD maxima (λ_{CT}), has been shown to be extremely sensitive to the nature of the axial ligands. Taken together with EPR data, this provides a discriminating assessment of heme axial ligation [13,21–23].

Four distinct low-spin Fe(III) heme species are apparent in the MCD spectra shown in Fig. 1. Each has a temperature-dependent near-IR MCD spectra indicative of transitions originating from an $S = 1/2$ ground state, and each can be correlated with a specific EPR signal. A summary of the λ_{CT} values and intensities and assignments for the dominant species is given in Table 1. Comparison of the cyt bc_1 and c_1 (pD 8) spectra shows that the $\lambda_{CT} = 1850$ nm component originates from the cyt c_1 species with the $g = 3.37$ low-field EPR feature. This is in the range established for hemes with histidine/methionine axial coordination (1740–1950 nm) and the low temperature MCD intensity under comparable conditions ($\Delta\epsilon = 180$–230 M^{-1} cm^{-1} at 4.2 K and 4.5 T) is similar to that reported for other hemes with histidine/methionine axial ligation ($\Delta\epsilon = 176$–330 M^{-1} cm^{-1} at 4.2 K and 5 T) [21,23]. The $\lambda_{CT} = 1590$ and 1660 nm components in the cyt bc_1 near-IR MCD spectra must therefore originate from the two b-type hemes in cyt b subunit. Preliminary MCD studies of samples poised at progressively lower potentials (data not shown) suggest that the $\lambda_{CT} = 1590$ and 1660 nm component correspond to cyt b_L and b_H, respectively. The latter is just outside the range established thus far for hemes with histidine/histidine (or histidine/imidazole) axial ligation (1500–1640 nm) [21,23]. However, the anomalously high MCD intensities ($\Delta\epsilon = 590$ M^{-1} cm^{-1} for cyt b_L and $\Delta\epsilon = 360$ M^{-1} cm^{-1} for cyt b_H, at 4.2 K and 4.5 T) [22], coupled with the HALS-type EPR spectra [12] and the mutagenesis results for the closely related bacterial complexes [14], all support *bis*-histidine ligation

Table 1
Near-IR VTMCD spectra and assignments for cyt bc_1 complexes and isolated cytochromes c_1

	Cyt b_L		Cyt b_H		Cyt c_1	
	λ_{CT} (nm)	$\Delta\epsilon$ (M^{-1} cm^{-1})	λ_{CT} (nm)	$\Delta\epsilon$ (M^{-1} cm^{-1})	λ_{CT} (nm)	$\Delta\epsilon$ (M^{-1} cm^{-1})
Bovine heart cyt bc_1	1590	590	1660	360	1850	180
Bovine heart cyt c_1 (pH 8)	1850	230				
Rb. sphaeroides cyt bc_1	1590	520	1660(sh)	310	1890	150
Rb. sphaeroides cyt c_1 (pH 8)	1520	180				
Rb. capsulatus cyt bc_1	1590	800	1650(sh)	450	1880	70
Rb. capsulatus cyt c_1 (pH 8)	1520	230				
R. rubrum cyt bc_1	1620	530	1670	360	1850	150

for both hemes with near-perpendicular arrangement of the imidazole rings. Hence the MCD results for cyt b_H serve to extend the range of λ_{CT} values for *bis*-histidine hemes to 1500–1660 nm. The MCD spectra for cyt c_1 at pD 10 and the pD 10 minus pD 8 difference spectra show that the cyt c_1 species with the $g = 2.95$ low-field EPR feature exhibits porphyrin(π)-to-Fe(III) charge transfer MCD bands with $\lambda_{CT} = 1510$ nm. This lies within the ranges established for histidine/histidine and histidine/amine (lysine or N-terminal amine) axial ligation, 1500–1640 nm and 1480–1550 nm, respectively, and close to the one example currently known of histidinate/methionine axial ligation, i.e., high-pH form of *E. coli* cyt b_{562}, $\lambda_{CT} = 1550$ nm [21]. The latter might be expected to exhibit a methionine(S)-to-Fe(III) charge transfer band close to 695 nm, but this was not apparent in the absorption or VTMCD spectra of cyt c_1 at pD 8 or pD 10.

3.2. Spectroscopic studies of Rb. sphaeroides cyt bc_1 complex and cyt c_1

Near-IR VTMCD spectra for oxidized *Rb. sphaeroides* cyt bc_1 complex and isolated cyt c_1 (pD 8) are shown in Fig. 3. Parallel low-temperature UV/visible absorption studies (1.6 K) on the identical samples confirmed that all cytochromes were all fully oxidized in both samples. EPR spectra of the samples used for VTMCD investigations, i.e., in a D_2O buffer with 53–57% (v/v) d_2-ethylene glycol are shown in Fig. 4. In addition, Fig. 4 shows EPR spectra for as prepared samples of the cyt bc_1 complex and cyt c_1, and for a cyt c_1 sample after exchange into a D_2O buffer, but before addition of ethylene glycol. The EPR spectra of the *Rb. sphaeroides* cyt bc_1 complex and cyt c_1 are in good agreement with the published data and the low-field components centered at $g = 3.78$, 3.49 and 3.36 are accordingly assigned to cyt b_L, cyt b_H and cyt c_1, respectively. In addition the samples used in this work showed an additional, slower-relaxing resonance with a low-field component at $g = 2.96$. EPR in this spectral region were not reported in previous studies. Such resonances are commonly observed for irreversibly denatured *b*-type hemes [36] and very similar spectra are observed for *bis*-imidazole Fe(III) porphyrin complexes which are devoid of the constraints of protein conformation [37]. Further evidence that this resonance originates from denatured hemes comes from the observation that it increases in intensity relative to that of the $g = 3.78$, 3.49 and 3.36 species with sample handling, e.g., compare spectra Fig. 4a and b. However, this is a minor component even in the cyt bc_1 samples used for VTMCD studies. Spin quantitation estimates for this sample, based on the area under the low-field absorption-shaped features under non-saturating conditions after correction for relative transition probabilities, indicate that the $g \approx 2.96$ species accounts for $\lesssim 40\%$ of the spin intensity of each of the other three components.

More dramatic effects on the EPR properties of cyt c_1 were observed when samples of the isolated cyt c_1 were prepared for VTMCD investigations, see Fig. 4c,d,e. As for cyt c_1 from bovine heart mitochondria, the EPR spectra are a mixture of two resonances with low-field components at $g = 3.36$ and 2.96. However, in contrast to bovine cyt c_1, the ratio of these two species in *Rb. sphaeroides* cyt c_1 was found to be very dependent on the extent of sample handling and the presence of the glassing agent (55% (v/v) d_2-ethylene glycol or d_3-glycerol). The relative concentration of the $g = 3.36$:$g = 2.96$ species was estimated as for bovine cyt c_1, see above, and varied from 4:1 in the as prepared sample (i.e., after one freeze-thaw cycle), to 2:3 after H_2O/D_2O buffer exchange, to $> 80\%$ $g = 2.96$ species after addition of d_2-ethylene glycol or glycerol. Formation of the $g = 2.96$ species was irreversible and independent of pH over the range 6–10. Samples exhibiting predominantly the $g = 3.36$ or the $g = 2.96$ species in the frozen EPR samples were fully reducible using excess ascorbate (1 mM) as judged by EPR studies of ascorbate reduced samples and comparative UV/visible absorption studies of oxidized, ascorbate-reduced and dithionite-reduced samples.

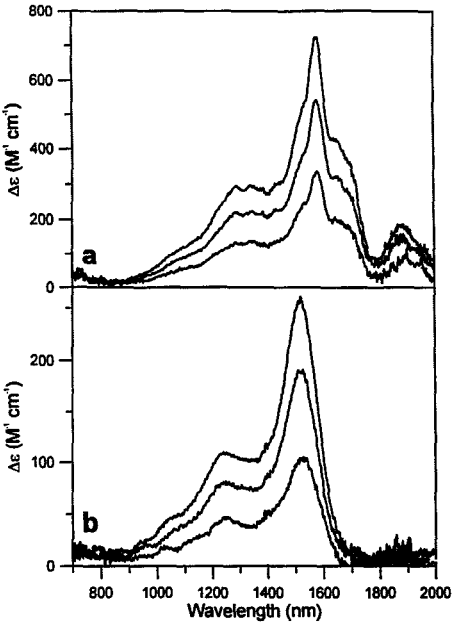

Fig. 3. VTMCD spectra of *Rb. sphaeroides* cyt bc_1 complex and isolated cyt c_1. (a) cyt bc_1 complex, 31 μM in 50 mM Tris-DCl buffer (pD 8.0), 400 mM NaCl, with 0.02% dodecyl maltoside and 53% d_2-ethylene glycol. Spectra recorded with an applied magnetic field of 4.5 T at 1.72 K, 4.22 K, and 8.9 K. (b) cyt c_1, 62 μM in 25 mM Tris-DCl buffer (pD 8.0), with 57% d_2-ethylene glycol. Spectra recorded with an applied magnetic field of 4.5 T at 1.64 K, 4.22 K and 9.5 K. All MCD bands increase in intensity with decreasing temperature.

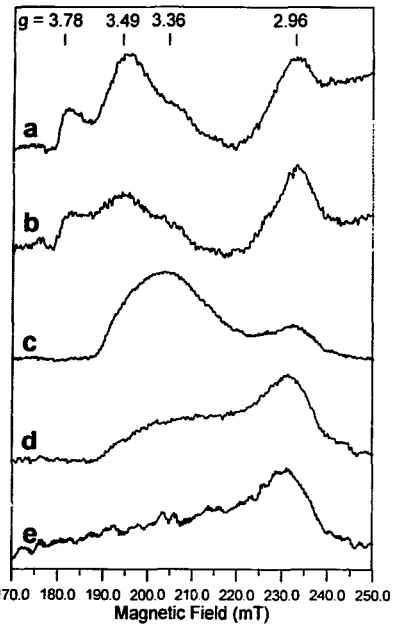

Fig. 4. EPR spectra of *Rb. sphaeroides* cyt bc_1 complex and isolated cyt c_1. (a) Cyt bc_1 complex, 66 μM in 15 mM Tris-HCl buffer (pH 8.0), 400 mM NaCl, with 0.01% dodecyl maltoside and 10% glycerol. (b) Cyt bc_1 complex, sample as used for VTMCD studies and described in Fig. 3. (c) Cyt c_1, 474 μM in 50 mM Tris-HCl buffer (pH 8.0). (d) cyt c_1, 130 μM in 50 mM Tris-DCl buffer (p*D* 8.0). (e) Cyt c_1 sample as used for VTMCD studies and described in Fig. 3. The spectra were recorded at 10 K and the instrument settings were: microwave power, 10 mW; modulation amplitude, 1.62 mT; microwave frequency 9.6 GHz.

The EPR results facilitated interpretation of the dramatic differences in the near-IR VTMCD properties of cyt c_1 in *Rb. sphaeroides* cyt bc_1 complex compared to the isolated protein, see Fig. 3, and in samples purified from bovine heart mitochondria compared to those purified from *Rb. sphaeroides*, cf. Fig. 1b and 3b, and Table 1. The near-IR VTMCD spectra for the *Rb. sphaeroides* cyt bc_1 complex are similar to those of the bovine cyt bc_1 complex and can be assigned by direct analogy, see Table 1. The major differences lie in a less well-defined band at 1660 nm from cyt b_H, a shift in the cyt c_1 λ_{CT} value to 1890 nm, and a more pronounced shoulder at ~ 1520 nm which is attributed to species responsible for the $g = 2.96$ EPR resonance. However, the intensity ($\Delta\epsilon = 150$ M^{-1} cm^{-1} at 4.2 K and 4.5 T) and wavelength of the charge transfer band at 1890 nm provides convincing evidence that the majority of the cyt c_1 in the *Rb. sphaeroides* cyt bc_1 complex has histidine/methionine axial ligation. In contrast, the purified cyt c_1 from *Rb. sphaeroides* is devoid of MCD bands in the 1740–1960 nm region that would be indicative of a heme with histidine/methionine axial ligation. Rather near-IR MCD spectrum indicates a homogeneous low-spin Fe(III) heme with $\lambda_{CT} = 1520$ nm. This MCD spectrum is clearly associated with the $g = 2.96$ EPR signal and is very similar to that deduced by difference techniques for the $g = 2.96$ species in alkaline bovine cyt c_1, cf. Figs. 1 and 3b. The close similarity in the EPR and MCD properties of the $g = 2.96$ species in bovine and *Rb. sphaeroides* cyt c_1 indicates similar axial ligation. As indicated above, the near-IR MCD properties are most consistent with histidine/histidine, histidine/amine, or histidinate/methionine axial ligation. Careful inspection of the absorption and VTMCD spectra gave no indication of a band close to 695 nm that might be associated with methionine(S)-to-Fe(III) charge transfer.

3.3. Spectroscopic studies of wild-type and the cyt c_1 M183L mutant of Rb. capsulatus cyt bc_1 complex and cyt c_1

Near-IR VTMCD spectra for oxidized *Rb. capsulatus* cyt bc_1 complex, wild-type and the cyt c_1 M183L mutant, and isolated cyt c_1 (p*D* 8) are shown in Fig. 5. Parallel low-temperature UV/visible absorption studies (1.6 K) on the identical samples confirmed that all cytochromes were fully oxidized in these samples. EPR spectra of fully oxidized samples of *Rb. capsulatus* cyt bc_1 complex (wild-type or M183L mutant) or isolated cyt c_1 have not been published previously and one of the objectives of this work was to characterize the EPR properties of cyt c_1 in this bacterial cyt bc_1 complex. Fig. 6 shows a comparison of the EPR spectra for the oxidized and ascorbate-reduced wild-type complex and the oxidized M183L mutant complex, in addition to EPR spectra of the MCD samples of the wild-type cyt bc_1 complex and purified cyt c_1 (i.e., in a D_2O buffer with 53–60% (v/v) d_2-ethylene glycol). EPR spectra of the *b*-type cytochromes in ascorbate-reduced samples of the *Rb. capsulatus* cyt bc_1 complex have been reported previously [28] and the results concur with those presented in Fig. 6, i.e., $g = 3.78$ and $g = 3.44$ components corresponding to cyt b_L and cyt b_H, respectively. Two additional low-field components of low-spin Fe(III) heme resonances were observed to higher field in the oxidized samples. One is an ascorbate-reducible component centered at $g = 3.16$. This resonance is also not observed in oxidized cyt bc_1 samples containing the cyt c_1 M183L mutation, which are devoid of a high-potential cyt c_1 [19]. Hence the $g = 3.16$ species is attributed to cyt c_1 in the intact cyt bc_1 complex. As for the *Rb. sphaeroides* cyt bc_1 samples, the *Rb. capsulatus* cyt bc_1 samples used in this work also exhibited a $g = 2.95$ resonance that is not ascorbate-reducible and is attributed to denatured *b*-type hemes. EPR spectra in this region were not shown in previously published spectra [28]. Spin quantitation estimates, based on the area under the low-field absorption-shaped features under non-saturating conditions after correction for the relative transition probabilities, indicate that

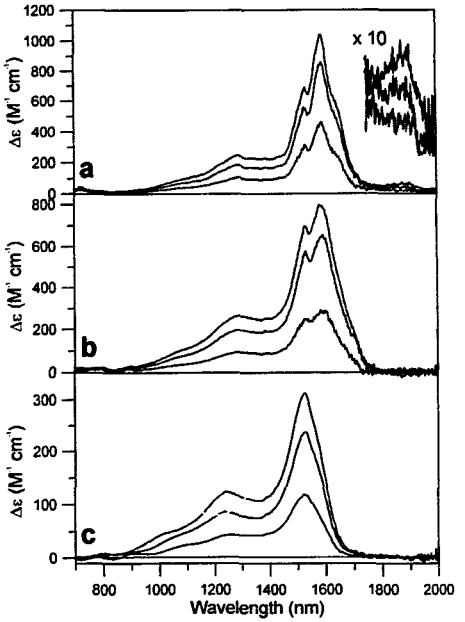

Fig. 5. VTMCD spectra of *Rb. capsulatus* cyt bc_1 complex, wild-type and cyt c_1 M183L mutant, and isolated cyt c_1. (a) Wild-type cyt bc_1 complex, 73 μM in 25 Tris-DCl buffer (p*D* 8.0), 100 mM NaCl, with 0.1% dodecyl maltoside and 55% d_2-ethylene glycol. Spectra recorded with an applied magnetic field of 4.5 T at 1.63 K, 4.22 K and 9.4 K. (b) Cyt c_1 M183L mutant of the cyt bc_1 complex, 80 μM in 25 Tris-DCl buffer (p*D* 8.0), 100 mM NaCl, with 0.1% dodecyl maltoside and 53% d_2-ethylene glycol. Spectra recorded with an applied magnetic field of 4.5 T at 1.59 K, 4.22 K and 10.5 K. (c) Cyt c_1, 114 μM in 50 mM Tris-DCl buffer (p*D* 8.0), 20 mM NaCl, 2 mM dithiothreitol, 2 mM EDTA, with 0.4% sodium cholate and 60% d_2-ethylene glycol. Spectra recorded with an applied magnetic field of 4.5 T at 1.64 K, 4.22 K and 9.7 K. All MCD bands increase in intensity with decreasing temperature.

the $g = 2.96$ resonance accounts for approximately 50% and the $g = 3.16$ resonance accounts for approximately 30% of the spin intensity of each of two *b*-type cytochromes.

The oxidized *Rb. capsulatus* cyt bc_1 sample used for MCD studies exhibited similar EPR spectra to the as prepared samples except for enhancement of the $g = 3.16$ species relative to the $g = 2.96$ species, cf. Fig. 6a and d, such that it corresponds to approximately 50% of the spin intensity of each of *b*-type cytochromes. The MCD sample of cyt c_1 from *Rb. capsulatus* showed only the $g = 2.96$ resonance with no indication of the $g = 3.16$ resonance attributed to cyt c_1 in the intact *Rb. capsulatus* cyt bc_1 complex. Indeed thus far we have been unable to observed the $g = 3.16$ resonance in any purified sample of *Rb. capsulatus* cyt c_1. Freshly prepared samples without added glassing agent and prior to D_2O/H_2O buffer exchange only exhibited the $g = 2.96$ resonance. However, the purified cyt c_1 samples are all completely reduced by ascorbate (1 mM), as judged by EPR and UV/visible absorption studies, and the EPR properties were invariant to pH over the range 8–10.

The near-IR VTMCD results for wild-type and the cyt c_1 M183L mutant form of *Rb. capsulatus* cyt bc_1 complex and cyt c_1, see Fig. 5 and Table 1, support and facilitate assignment of the EPR results and provide insight into the axial ligation of cyt c_1 in the M183L mutant. The wild-type and cyt c_1 M183L mutant cyt bc_1 complexes have components with $\lambda_{CT} = 1590$ nm and 1650 nm (shoulder) that are attributed to cyt b_L an cyt b_H, respectively, by analogy with the bovine and *Rb. sphaeroides* cyt bc_1 complexes. The shoulder at 1520 nm is more pronounced than in the bovine or *Rb. sphaeroides* cyt bc_1 complexes which is consistent with the increased intensity in the $g = 2.95$ resonance. Moreover, the relative intensity of this feature is dramatically enhanced in the M183L mutant, indicating

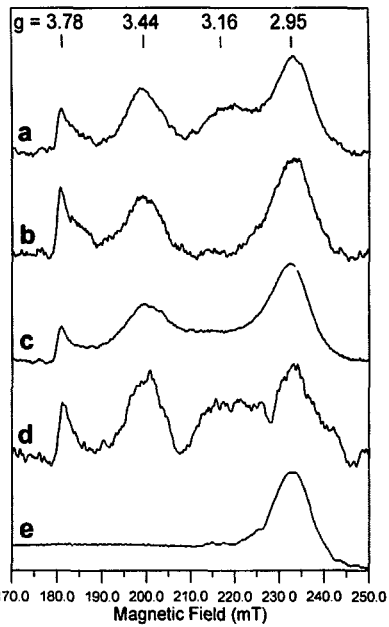

Fig. 6. EPR spectra of *Rb. capsulatus* cyt bc_1 complex, wild-type and cyt c_1 M183L mutant, and isolated cyt c_1. (a) Wild-type cyt bc_1 complex, 100 μM in 50 mM Tris-HCl buffer (pH 8.0), 200 mM NaCl, with 0.2% dodecyl maltoside. (b) Ascorbate-reduced wild-type cyt bc_1 complex, as described in (a) with 1.5 mM ascorbate. (c) Cyt c_1 M183L mutant of the cyt bc_1 complex, 100 μM in 50 mM Tris-HCl buffer (pH 8.0), 200 mM NaCl, with 0.2% dodecyl maltoside. (d) Wild-type cyt bc_1 complex, sample as used for VTMCD studies and described in Fig. 5. (e) Cyt c_1, sample as used for VTMCD studies and described in Fig. 5. The spectra were recorded at 10 K and the instrument settings were: microwave power, 10 mW; modulation amplitude, 1.62 mT; microwave frequency 9.6 GHz.

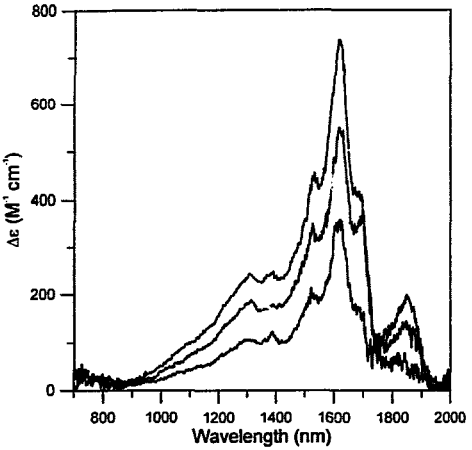

Fig. 7. VTMCD spectra of *R. rubrum* cyt bc_1 complex. Cyt bc_1 complex, 43 μM in 35 mM MOPS buffer (pH 7.4), 1 mM $MgSO_4$, with 0.2% dodecyl maltoside and 55% d_2-ethylene glycol. Spectra recorded with an applied magnetic field of 4.5 T at 1.64 K, 4.22 K and 8.7 K.

that cyt c_1 in this mutant has $\lambda_{CT} = 1520$ nm and is responsible at least in part for the $g = 2.95$ resonance. The wild-type sample has a weak MCD band with $\lambda_{CT} = 1880$ nm that is indicative of a heme with histidine/methionine axial ligation and assigned to the ascorbate-reducible $g = 3.16$ resonance. In accord with the low relative intensity of the $g = 3.16$ species in the EPR spectrum, the MCD band is approximately half the intensity of the equivalent band in the *Rb. sphaeroides* cyt bc_1 complex. The MCD sample of the purified cyt c_1 shows no indication of a heme with histidine/methionine axial ligation and exhibits solely the $\lambda_{CT} = 1520$ nm MCD spectrum that is the hallmark of the $g = 2.96$ species. It appears that the spectroscopic properties of the form of *Rb. capsulatus* cyt c_1 that exhibits the $g = 2.96$ resonance are very similar to the form of cyt c_1 induced via the M183L mutation. However, they must differ in terms of their midpoint potential since cyt c_1 is not reduced by ascorbate in the cyt bc_1 samples containing the M183L mutation in cyt c_1 [19].

3.4. VTMCD studies of the R. rubrum cyt bc_1 complex

Near-IR VTMCD spectra for the *R. rubrum* cyt bc_1 complex are shown in Fig. 7 and summarized in Table 1. Insufficient sample was available for parallel EPR studies. Nevertheless, the MCD data provide strong evidence that this complex has at least four distinct low-spin Fe(III) hemes and rational assignments can be made based on the resulted presented above for mitochondrial and bacterial cyt bc_1 complexes: $\lambda_{CT} = 1620$ nm, cyt b_L: $\lambda_{CT} = 1670$ nm (shoulder), cyt b_L: $\lambda_{CT} = 1850$ nm, cyt c_1: $\lambda_{CT} = 1520$ nm, denatured *b*-type and possibly c_1-type cytochromes. The intensity of the 1850 nm band, as compared with the other cyt bc_1 complexes investigated herein, is consistent with the majority of the cyt c_1 having histidine/methionine axial ligation in the intact complex.

3.5. Properties of N-terminal-acetylated Rb. capsulatus c_1

Recent x-crystallographic data have established histidine/N-terminal amine axial ligation for cyt *f* in the chloroplast cyt b_6f complex, which is functionally equivalent to cyt c_1 in the cyt bc_1 complex. The possibility of this type of coordination in bacterial cyts c_1 prompted an investigation of the properties of *Rb. capsulatus* cyt c_1 acetylated at the N-terminus.

Rb. capsulatus cyt c_1, separated from the intact cyt bc_1 complex and purified as described in Section 2, showed a single Coomassie-staining band with an apparent M_r of 29000, after polyacrylamide gel electrophoresis in the presence of SDS, and a single band in isoelectric focusing (p*I* = 5.6). These observations and the pattern observed during amino acid sequencing of the protein (see below), suggest that the cyt c_1 samples used in these experiments are > 90% pure. In its reduced form, the purified *Rb. capsulatus* cyt c_1 has α-band, β-band and Soret-band absorbance maxima at 552.5 nm, 523.5 nm and 417.5 nm, respectively. The α- and β-bands are shown in Fig. 8. These α-band and β-band maxima are essentially identical to those for the cyt c_1 in the intact *Rb. capsulatus* cyt bc_1 complex [28]. Spectrophotometric redox titrations indicate an E_m value for the isolated, purified cyt c_1 of + 260 ± 10 mV, see Fig. 9, close to the value of + 290 mV reported

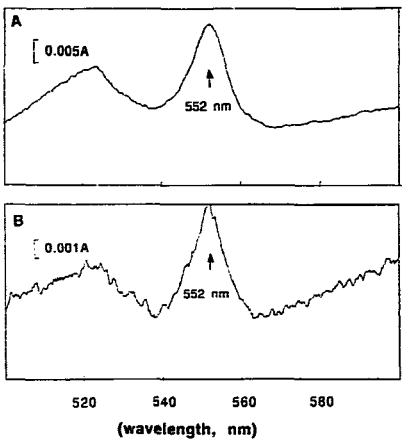

Fig. 8. Reduced *minus* oxidized difference absorption spectra for native and acetylated *Rb. capsulatus* cyt c_1. The reaction mixture contained either native *Rb. capsulatus* cyt c_1 (upper panel) at a concentration of 19.4 μM, or acetylated *Rb. capsulatus* cyt c_1 (lower panel) at a concentration of 9.1 μM, in 10 mM potassium phosphate buffer (pH 7.4) containing 0.25% sodium cholate.

for the cyt c_1 in the intact *Rb. capsulatus* cyt bc_1 complex [28].The isolated *Rb. capsulatus* cyt c_1, like the intact *Rb. capsulatus* cyt bc_1 complex [38], co-chromatographs with *Rb. capsulatus* cyt c_2 during gel filtration chromatography at low ionic strength, but not at high ionic strength (data not shown), indicating that separation of the *Rb. capsulatus* cyt c_1 from the other subunits of the cyt bc_1 complex does not eliminate its ability to form an electrostatically stabilized complex with its physiological electron acceptor.

The gene, referred to as *pet*C, coding for cyt c_1 in the *Rb. capsulatus* strain used in these experiments had been sequenced previously [39]. However, this gene codes for a precursor form that is larger than the mature form of the cytochrome [39] and the exact cleavage site for the cyt c_1 leader sequence had not been definitively established. We have determined that the amino acid sequence of the first 20 amino acids at the amino-terminal region of the isolated, purified *Rb. capsulatus* cyt c_1 is NSNVPDHAFSFEGIFGKYDQ, in exact agreement with that predicted from the nucleotide sequence [39], if a 21-amino-acid leader sequence is cleaved off during processing of the cytochrome. It should be noted that an identical leader sequence cleavage site, leaving asparagine as the N-terminal amino acid of the mature cyt c_1, was reported previously for the cyt c_1 [40] that was erroneously identified as a *Rb. sphaeroides* protein, but which, in fact, was from an unidentified strain of *Rb. capsulatus* [41].

Rb. capsulatus cyt c_1, acetylated as described in Materials and Methods, shows three Coomassie-staining bands after isoelectric focusing (data not shown), only one of which had a p*I* significantly lower than that of the unacetylated control. This indicates that the acetylated sample was a mixture of cyt c_1 acetylated to different degrees, with most of the protein acetylated to a small extent. Nevertheless, acetylation at the N-terminus was essentially complete, as documented by the observation that the protein was at least 91% blocked in amino acid sequencing trials, see Fig. 10. Blocking the N-terminal α-amino group of *Rb. capsulatus* cyt c_1 by acetylation had essentially no effect on the either the α-band and β-band regions, see Fig. 8, or on the E_m value of the cytochrome, see Fig. 9. Acetylation did not decrease the reduced *minus* oxidized extinction coefficient for the cytochrome in the α-band region and, in fact, may have increased it somewhat. Values of 15.9 ± 1.0 and 18.5 ± 1.0 mM^{-1} cm^{-1} for the reduced *minus* oxidized extinction coefficient at 552.5 nm were determined, based on alkaline pyridine hemochromagen determinations of the total heme present [42], for the control and acetylated cytochromes, respectively. While the quantities of acetylated cyt c_1 obtained were insufficient for meaningful EPR and VTMCD analyses, the observation that acetylation of more than 90% of the α-amino group of the N-terminal asparagine of *Rb. capsulatus* cyt c_1 had no effect on either the absorbance spectrum or E_m value, strongly suggests that, unlike cyt *f* [18], the N-terminal amino group does serve as a ligand to the heme of *Rb. capsulatus* cyt c_1.

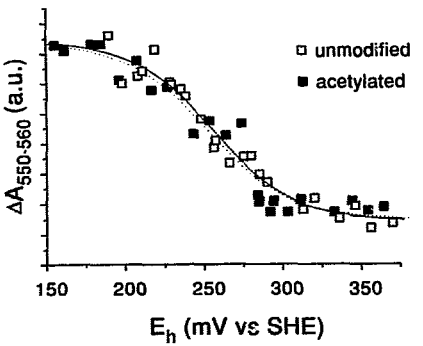

Fig. 9. Oxidation-reduction titrations of *Rb. capsulatus* cyt c_1. The reaction mixture contained either native (□) or acetylated (■) *Rb. capsulatus* cyt c_1 at a concentration of 5.7 μM in 50 mM Tris-HCl buffer (pH 7.0), containing 100 mM NaCl and 0.1 mg/ml dodecyl maltoside. The following mediator dyes were also present: 25 μM 2,5-dihydroxy-*p*-benzoquinone, 35 μM diaminodurene, 25 μM 1,2-naphthoquinone and 25 μM phenazine methosulfate. The solid and dashed lines represent the best fits for single components that follow the Nernst equation for a one-electron carrier for the acetylated and native samples, respectively.

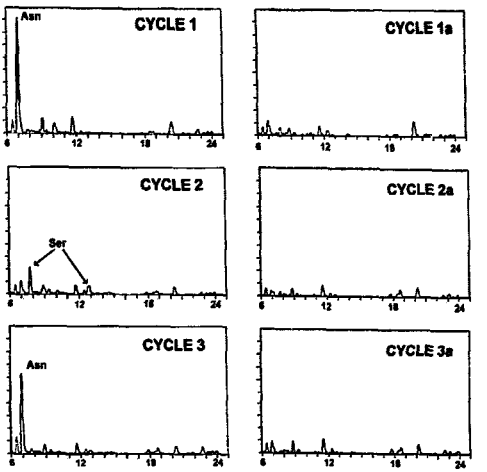

Fig. 10. Amino acid sequencing of native and acetylated *Rb. capsulatus* cyt c_1. The left-hand column shows the data obtained for the native, unmodified protein and the right-hand column the data obtained for the acetylated sample. 194 pmol of protein was loaded in each case.

4. Discussion

The results presented herein represent the first near-IR VTMCD study of any intact cyt bc_1 complex and demonstrate the utility of this technique, when combined with

parallel EPR studies, for identifying the axial ligation of hemes in multicytochrome complexes. For intact cyt bc_1 complexes, the results confirm the axial ligation of the individual cytochromes deduced from mutagenesis and EPR studies, i.e., *bis*-histidine axial ligation for cyt b_L (λ_{CT} = 1590–1620 nm, $\Delta\epsilon$ = 520–800 M^{-1} cm^{-1} at 4.2 K and 4.5 T) and cyt b_H (λ_{CT} = 1650–1670 nm, $\Delta\epsilon$ = 310–450 M^{-1} cm^{-1} at 4.2 K and 4.5 T), and histidine/methionine axial ligation for cyt c_1 (λ_{CT} = 1850–1890 nm, $\Delta\epsilon$ = 140–180 M^{-1} cm^{-1} at 4.2 K and 4.5 T). Near-perpendicular orientation of the histidine imidazole rings is responsible for the HALS-type EPR spectra and the anomalously high intensity of the porphyrin(π)-to Fe(III) charge transfer transitions in the near-IR VTMCD spectra of the cyts *b*. The properties of cyt c_1 in the *Rb. capsulatus* cyt bc_1 complex are somewhat anomalous compared to the other three cyt bc_1 complexes investigated in this work. The low field component of the EPR signal is centered at g = 3.16 compared to g = 3.37 and 3.36 in the bovine heart and *Rb. sphaeroides* cyt bc_1 complexes, respectively, and the near-IR MCD and EPR results taken together indicate that approximately half of *Rb. capsulatus* cyt bc_1 complex used in these studies has a cyt c_1 with histidine/methionine axial ligation. Since the purified samples of all the cytochromes c_1 investigated in this work all show evidence of two forms which differ in terms of heme axial ligation, it seems likely that cyt c_1 heterogeneity is the most probable reason for the substoichiometric amounts of histidine/methionine cyt c_1 in *Rb. capsulatus* cyt bc_1.

The bacterial cyt bc_1 complexes investigated in this work, but not the bovine heart cyt bc_1 complex, showed evidence for the presence some denatured *b*-type cytochromes which are characterized by a g = 2.95 EPR signal and near-IR MCD bands with λ_{CT} = 1520 nm. These spectroscopic properties are similar to those of *bis*-imidazole Fe(III) porphyrins, imidazole derivatives of myoglobin and horse heart cyt *c*, and many *bis*-histidine hemoproteins [21–23]. Hence the changes in MCD and EPR properties are attributed to subunit denaturation and/or dissociation within the cyt bc_1 complex leading to relaxation of the near-perpendicular arrangement of the histidine imidazole ring of the *b*-type cytochromes. However, the present work clearly demonstrates that both *b*-type and c_1-type hemes can be responsible for species exhibiting g = 2.95 EPR signals with λ_{CT} = 1520 nm. This species is found in varying amounts in purified samples of bovine heart, *Rb. capsulatus* and *Rb. sphaeroides* cyt c_1. It appears to form irreversibly at the expense of the histidine/methionine cyt c_1 that is present in the intact cyt bc_1 complexes, as a result of sample handling (i.e., freezing/thawing and buffer exchange), the addition of 50% (v/v) ethylene glycol or glycerol, or, at least in the case of bovine heart cyt c_1, a shift to more alkaline pH. (While results are presented only for samples treated with ethylene glycol, identical results were observed within experimental error for samples containing 50–60% glycerol.) Moreover, a form of cyt c_1 with very similar spectroscopic properties is present in the mutant *Rb. capsulatus* cyt bc_1 complex in which the coordinating methionine has been replaced by leucine (M183L mutant). The cyt c_1 from *Rb. capsulatus* shows the greatest propensity for conversion to the g = 2.95 species and we have as yet been unable to identify the form with histidine/methionine axial ligation in purified samples. In light of the intensity of the g = 2.95 resonance in the EPR and the λ = 1520 nm feature in the MCD of the *Rb. capsulatus* cyt bc_1 complex, it seems likely that the g = 2.95 form of cyt c_1 is present even in the intact complex and that both *b*- and c_1-type cytochromes contribute to these features.

From the above discussion, it is evident that the spectroscopic data for the g = 2.95 form of the cyt c_1 complex are consistent with *bis*-histidine axial ligation and hence the replacement of the ligating methionine by a histidine residue. Further support for this interpretation comes from the observation that the spectroscopic properties are almost identical to those in the F82H mutant of yeast cyt *c* (g = 2.96, 2.26, 1.51 and λ_{CT} = 1510 nm) in which the coordinated methionine (Met-80) is replaced by His-82 [43]. Despite the remarkable similarity in spectroscopic properties, the cyt c_1 and cyt *b*-derived g = 2.95 species differ in terms of midpoint potential. While more work is required to obtain precise E_m values, purified samples of *Rb. capsulatus* and *Rb. sphaeroides* cyt c_1 containing exclusively the g = 2.95 form are completely reducible by ascorbate, whereas cyt c_1 in the M183L mutant of *Rb. capsulatus* cyt bc_1 complex and the denatured *b*-type cytochromes are not ascorbate-reducible. This difference in midpoint potentials does not necessarily dictate differences in axial ligation, since it is clear that the heme environment as well as the nature of the axial ligands plays an important role in determining the midpoint potential [44,45]. However, it is worthwhile considering alternative axial ligation possibilities for the g = 2.95 form of cyt c_1.

Among the known types of axial heme ligation, histidinate/methionine and histidine/amine (lysine or N-terminal amine) are both viable alternatives to *bis*-histidine for the g = 2.95 form of cyt c_1, based on the near-IR MCD data, λ_{CT} = 1520 nm [21–23]. To our knowledge there is only one well characterized example of histidinate/methionine axial ligation, *E. coli* cyt b_{562} at p*D* 10.5, which has λ_{CT} = 1520 nm and g = 2.79, 2.26, and 1.67 [21]. Clearly without a wider range of examples, this type of axial coordination cannot be ruled out based on spectroscopic data alone. Furthermore in the case of purified bovine heart cyt c_1, the g = 2.95 form only appears at alkaline pH (p*D* 10.0). There are three main arguments against histidinate/methionine axial ligation: (1) conversion to the g = 2.96 form appears to be irreversible; (2) the histidine/methionine form was not recovered on lowering the pH (down to p*D* 6.0); (3) a species with very similar spectroscopic properties is observed in M183L

mutant. Generally the absence of a 695 nm in the VTMCD and absorption spectra would be convincing evidence against axial ligation by methionine, but the near absence of such a band for purified cyts c_1 which are predominantly in the histidine/methionine form shows that this is unlikely to be a reliable criterion in this instance.

The studies of the N-terminal acetylated *Rb. capsulatus* cyt c_1 provide no indication that the N-terminal amine is involved with axial heme coordination as has been shown to be the case in cyt *f* [18]. Moreover, the EPR properties of $g = 2.95$ form of cyt c_1 are quite distinct from known examples of ferrihemes with histidine/amine (lysine, N-terminal amine, or exogenous amine) which have HALS-type resonances with $g \geq 3.3$ [21,24,25]. Hence, it is unlikely that the heterogeneity in purified samples of cyt c_1 is related in any way to the alkaline transition of cyt *c* which has been show to be associated with replacement of coordinated methionine by an adjacent lysine at alkaline pH [46].

The results presented herein provide evidence for two forms of cyt c_1 that differ in terms of axial ligation, histidine/methionine *versus bis*-histidine. Both are high potential ($> +150$ mV), since they are completely reduced by ascorbate. The histidine/methionine form dominates in intact cyt bc_1 preparations and it seems likely that the *bis*-histidine form is an artifact of dissociation of cyt c_1 from the cyt bc_1 complex, coupled with medium effects on the structure of the solubilized subunit. A similar *bis*-histidine form of cyt c_1, albeit with a lower midpoint potential ($E_m = -74$ mV [19]), appears to be assembled in the M183L mutant of the *Rb. capsulatus* cyt bc_1 complex in which the methionine residue coordinating cyt c_1 is replaced by a leucine. The propensity for conversion to the *bis*-histidine form varies for different wild-type cyts c_1 (bovine heart < *Rb. sphaeroides* ≈ *R. rubrum* < *Rb. capsulatus*) Inspection and computer assisted alignments of the sequences of these cyt c_1, does not reveal a second conserved histidine that could be a candidate for the new ligand. However, several histidines are available and it may be significant that both *R. rubrum* and *Rb. capsulatus* cyt c_1 have histidines in close proximity to the coordinating methionine; H-X_3-M and H-X_5-M, respectively. Whether or not the *bis*-histidine form is functional for electron transport in wild-type cyt bc_1 complexes remains to be established. Overall, the results serve to emphasize the importance of spectroscopic studies on intact membrane-bound complexes, and show that purification and medium effects, particularly the addition of 50% (v/v) ethylene glycol or glycerol, can alter the axial ligation of cyt c_1.

Acknowledgements

This work was supported by grants from the National Institutes of Health (GM51962 to M.K.J., GM 30721 to C.-A.Y. and GM38237 to F.D.) and the US Department of Agriculture (93-37306-9084 to D.B.K.). Spectroscopic instrumentation was purchased in part with funds from the National Science Foundation (DIR9014281 and DIR9102055 to M.K.J.). Amino-acid sequencing was carried out in the Texas Tech University Biotechnology Institute Core Facility using equipment purchased with contributions from Texas Tech University and the National Science Foundation.

References

[1] Brandt, U. and Trumpower, B. (1994) Crit. Rev. Biochem. Mol. Biol. 29, 165–197.
[2] Yu, C.-A. and Yu., L. (1993) J. Bioenerg. Biomembr. 23, 259–273.
[3] Gennis, R.B., Barquera, B., Hacker, B., van Doren, S.R., Arnaud, S., Crofts, A.R., Davidson, E., Gray, K.A. and Daldal, F. (1993) J. Bioenerg. Biomembr. 25, 195–209.
[4] Knaff, D.B. (1993) Photosyn. Res. 35, 117–133.
[5] Malkin, R. (1992) Photosyn. Res. 33 121–136.
[6] Trumpower, B.L. (1990) Microbiol. Rev. 54, 101–129.
[7] Hauska, G., Nitschke, W. and Herrmann, R.G. (1988) J. Bioenerg. Biomembr. 20, 211–228.
[8] Crofts, A.R. and Wang, Z. (1989) Photosyn. Res. 22, 69–87.
[9] Britt, R.D., Sauer, K., Klein, M.P., Knaff, D.B., Kriauciunas, A., Yu., C.-A., Yu., L. and Malkin, R. (1991) Biochemistry 30, 1892–1901.
[10] Gurbiel, R.J., Ohnishi, T., Robertson, D.E., Daldal, F. and Hoffman, B.M. (1991) Biochemistry 30, 11579–11584.
[11] Davidson, E., Ohnishi, T., Atta-Asafo-Adjei, E. and Daldal, F. (1992) Biochemistry 31, 3342–3351.
[12] Salerno, J.C. (1984) J. Biol. Chem. 259, 2331–2336.
[13] Simpkin, D., Palmer, G., Devlin, F.J., McKenna, M.C., Jensen, G.M. and Stephens, P.J. (1989) Biochemistry 28, 8033–8039.
[14] Yun, C.-H., Crofts, A.R. and Gennis, R.B. (1991) Biochemistry 30, 6747–6754.
[15] Salerno, J.C., McCurley, J.P., Dong, J.-H., Doyle, M.F., Yu., L. and Yu, C.-H. (1986) Biochem. Biophys. Res. Commun. 136, 616–621.
[16] McCurley, J.P., Miki, T., Yu, L. and Yu, C.-A. (1990) Biochim. Biophys. Acta 1020, 176–186.
[17] Lou, B.-S., Hobbs, J.D., Chen, Y.-R., Yu, L., Yu, C.-A. and Ondrias, M.R. (1993) Biochim. Biophys. Acta 1144, 403–410.
[18] Martinez, S.E., Huang, D., Szczepaniak, A., Cramer, W.A. and Smith, J.L. (1994) Structure 2, 95–105.
[19] Gray, K.A., Davidson, E. and Daldal, F. (1992) Biochemistry 31, 11864–11873.
[20] Nakai, M., Ishiwatari, H., Asada, A., Bogaki, M., Kawai, K., Tanaka, Y. and Matsubara, H. (1990) J. Biochem. 108, 798–803.
[21] Gadsby, P.M.A. and Thomson, A.J. (1990) J. Am. Chem. Soc. 112, 5003–5011.
[22] Thomson, A.J. and Gadsby, P.M.A. (1990) J. Chem. Soc., Dalton Trans, 1921–1928.
[23] Cheesman, M.R., Greenwood, C. and Thomson, A.J. (1991) Adv. Inorg. Chem.36, 201–255.
[24] Gadsby, P.M.A., Peterson, J., Foote, N., Greenwood, C. and Thomson, A.J. (1987) Biochem J. 246, 43–54.
[25] Rigby, S.E.J., Moore, G.R., Gray, J.C., Gadsby, P.M.A., George, S.J. and Thomson, A.J. (1988) Biochem. J. 256, 571–577.
[26] Güner, S., Robertson, D.E., Yu., L., Qiu, Z., Yu, C.-A. and Knaff, D.B. (1991) Biochim. Biophys. Acta 1058, 269–279.
[27] Yu., L., Mei, Q.-C. and Yu, C.-A. (1984) J. Biol. Chem. 259, 5752–5760.

[28] Robertson, D.E., Ding, H., Chelminski, P.R., Slaughter, C., Hsu, J., Moomaw, C., Tokito, M., Daldal, F. and Dutton, P.L. (1993) Biochemistry 323, 1310–1317.
[29] Yu, C.-A., Chiang, Y.-L., Yu, L. and King, T.E. (1975) J. Biol. Chem. 250, 6216–6221.
[30] Yu, L., Dong, J.-H. and Yu, C.-A. (1986) Biochim. Biophys. Acta 852, 203–211.
[31] Takemori, S., Wada, K., Ando, K., Hosokawa, M., Sekuzu, I. and Okunuki, K. (1962) J. Biol. Chem. 52, 28–37.
[32] Dutton, P.L. (1978) Methods Enzymol. 54, 411–435.
[33] Johnson, M.K. (1988) in Metal Clusters in Proteins (Que, L., ed.), ACS Symposium Series, Vol. 372, pp. 326–342, American Chemical Society, Washington, DC.
[34] Thomson, A.J., Cheesman, M.R. and George, S.J. (1993) Methods Enzymol. 226, 199–232.
[35] DeVries, S. and Albracht, S.P.J. (1979) Biochim. Biophys. Acta 546, 334–340.
[36] Salerno, J.C., McGill, J.W. and Gerstle, G.C. (1983) FEBS Lett. 162, 257–261.
[37] Salerno, J.C. and Leigh, J.S. (1984) J. Am. Chem. Soc. 106, 2156–2159.
[38] Güner, S., Willie, A., Millett, F., Caffrey, M.S., Cusanovich, M.A., Robertson, D.E. and Knaff, D.B. (1993) Biochemistry 32, 4793–4800.
[39] Davidson, E. and Daldal, F. (1987) J. Mol. Biol. 195, 13–24.
[40] Gabellini, N. and Sebald, W. (1986) Eur. J. Biochem. 154, 569–579.
[41] Davidson, E. and Daldal, F. (1987) J. Mol. Biol. 195, 25–29.
[42] Drabkin, D.L. (1942) J. Biol. Chem. 146, 605–617.
[43] Hawkins, B.K., Hilgen-Willis, S., Pielak, G.J. and Dawson, J.H. (1994) J. Am. Chem. Soc. 116, 3111–3112.
[44] Cusanovich, M.A., Meyer, T.E. and Tollin, G. (1987) in Advances in Inorganic Biochemistry (Eichorn, G.C. and Marzilli, L.G., eds.), Vol. 7, pp. 37–92, Elsevier, New York.
[45] Moore, G.R. and Pettigrew, G.W. (1990) in Cytochromes *c*, Evolutionary, Structural and Physiocochemical Aspects, Springer, New York.
[46] Ferrer, J.C., Guillemette, J.G., Bogumil, R., Inglis, S.C., Smith, M. and Mauk, A.G. (1993) J. Am. Chem. Soc. 115, 7507–7508